Monthly Weather Review

VOLUME 99, NUMBER 11

NOVEMBER 1971

UDC 551.576:551.521.14:551.507.362.2:535-1

ESTIMATION OF THE EFFECT OF PARTIAL CLOUD COVER ON THE RADIATION RECEIVED BY THE NIMBUS HRIR

FRED M. VUKOVICH

Research Triangle Institute, Research Triangle Park, N.C.

ABSTRACT

A theoretical technique was employed to compute the magnitude of the effect of cloud interference on the Nimbus High Resolution Infrared Radiometer (HRIR) data. A comparative study using HRIR and ground truth data suggests that the derived results could be used successfully as an analysis tool to discriminate cloud-contaminated temperatures from clear-sky temperatures provided an estimate of the cloud cover and type is available.

1. INTRODUCTION

The degree to which clouds absorb radiation emitted from the earth's surface in the wavelength band (3.5–4.1 μm) employed by the Nimbus High Resolution Infrared Radiometer (HRIR) depends on the cloud cover over the area. Total cloud cover (overcast) absorbs all radiation emitted from the earth's surface since clouds are approximately blackbodies. An overcast is readily detectable in Nimbus HRIR data and does not produce any analysis difficulty but does create a surface data void. As the cloud cover decreases, it becomes increasingly difficult to distinguish cloud-contaminated areas from clear-sky areas through their respective radiation signatures. This is especially true for cloud cover of 0.3 or less. In that range, temperatures and temperature patterns for the sea surface under clear skies, for instance, are not easily distinguishable from cloud-contaminated temperatures and temperature patterns (Allison et al. 1967, Bandeen 1969, Krishna Rao 1968, Vukovich and Blanton 1969). It is important, therefore, that some method of dealing with partial cloud cover be found to allow accurate analysis of the Nimbus HRIR data. A technique is presented by which an estimate of the temperature reduction produced by clouds can be made.

2. PROCEDURE

The "cloud temperature difference," δT, is defined as the difference between the equivalent blackbody temperature that would be observed by a satellite under clear skies and for a given nadir angle, and the equivalent blackbody temperature that would be observed by the same satellite at the same nadir angle, but with a given percent cloud cover obstructing the view, and a given cloud top height. A modified form of the solution to the radiative transfer equation (Vukovich 1970) was used to compute the monochromatic radiation received by a satellite with partly cloudy skies, N_λ, that is

$$N_\lambda = \phi_\lambda \left\{ \tau'_\lambda [(1-\alpha)R_\lambda + \alpha E_\lambda(T_c)] + \int_{p_c}^{p_s} E_\lambda(T) \frac{\partial \tau_\lambda}{\partial p} dp \right\} \quad (1)$$

where ϕ_λ is the spectral response of the radiometer; τ'_λ is the spectral transmissivity in the layer p_c to p_s; p_c is the pressure at which the cloud top is found; p_s is the pressure at which the satellite is found; α is the percent cloud cover in the area, A, projected by the solid angle subtended from the satellite to the radiating surface; T_c is the temperature at the cloud top; T is temperature; τ_λ is the spectral transmission function; λ is wavelength; $E_\lambda(T)$ is the Planck function; and p is pressure. The clouds are assumed to be blackbodies and to be uniformly distributed in the area.

The last term on the right (the pressure integral term) is the contribution to the average spectral radiance from the atmosphere in the layer p_c to p_s. The term $\alpha E_\lambda(T_c)$ is the emitted blackbody radiance from the part of the area at p_c covered by clouds. The term $(1-\alpha)R_\lambda$ is the portion of the radiation, R_λ, emitted from pressure surfaces greater than p_c passing through p_c in the clear part of the area. The spectral radiance, R_λ, also can be defined through the solution of the radiative transfer equation,

$$R_\lambda = \epsilon_\lambda \tau'_\lambda{}' E_\lambda(T_0) + \int_{p_0}^{p_c} E_\lambda(T) \frac{\partial \tau_\lambda}{\partial p} dp. \quad (2)$$

In deriving eq (2), the emissivity, ϵ_λ, and the temperature, T_0, of the earth's surface at pressure, p_0, were assumed constant in the projection of the area, A, to the surface.

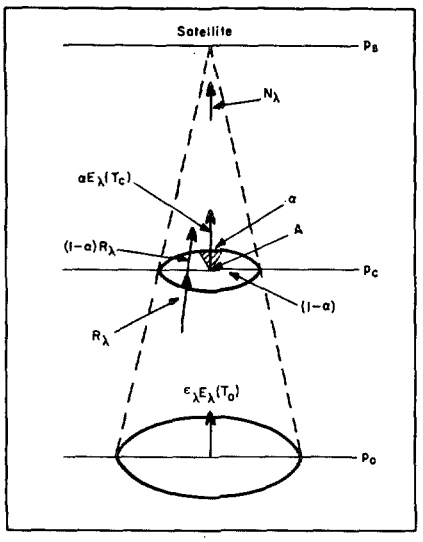

FIGURE 1.—Schematic diagram depicting the theory used to compute the amount of radiation attenuated by partial cloud cover.

The term τ_λ'' is the clear-sky, spectral transmissivity in the layer p_0 to p_c (no clouds present in the layer). The first term on the right is the radiation received at p_c emitted from the surface, and the second term is the radiation received at p_c emitted by the atmosphere in the layer between p_0 and p_c.

The radiative process under partial cloud cover may be summarized as follows (fig. 1). Part of the radiation emitted from the earth's surface, $[\epsilon_\lambda E_\lambda(T_0)]$, and from the atmosphere in the layer from the surface to the cloud top, is absorbed by the clouds that are in the volume defined by the satellite's field of view. The remainder passes through that portion of the volume unobstructed by clouds, $[(1-\alpha)R_\lambda]$, and makes up a fraction of the average spectral radiance observed by the satellite (N_λ). The remaining contributions to the average spectral radiance originate from the radiation emitted by the clouds, $[\alpha E_\lambda(T_c)]$, with tops that are uniformly found at pressure p_c, and from the radiation emitted by the atmosphere in the layer from the cloud top to the satellite. For the Nimbus HRIR, the total radiance, N, received by the satellite is defined as

$$N=\int_{\lambda_1}^{\lambda_2} N_\lambda d\lambda \tag{3a}$$

where λ_1 and λ_2 are 3.5 and 4.1μm, respectively.

To solve these equations, we constructed a 20-level model that had upper and lower boundaries at the 20- and 100-cb levels, respectively. No significant absorption of radiant energy was found at pressures less than 20 cb for the HRIR wavelength band (Vukovich and Blanton 1969); so the model essentially computed the radiant energy received by the satellite. The layer between 20 and 100 cb was divided into levels 4 cb apart. Water vapor and carbon dioxide were the only absorbing gases accounted for in the model (Kunde 1965). The calculations were made using the temperature and water vapor distribution for each of three atmospheres: polar, tropical, and Standard Atmosphere. The water vapor distribution was obtained by assuming that the atmosphere was saturated. The carbon dioxide was assumed uniformly mixed in the atmosphere and the mixing ratio was 0.5 g·kg^{-1}. The earth's surface was treated as a blackbody ($\epsilon_\lambda=1.0$), and the HRIR spectral response was obtained from the Nimbus 2 User's Guide (1966). The cloud cover, α, was allowed to vary from 0.1 to 0.9, and the cloud tops varied from near the surface to 10 km. For a given cloud top height, the temperature obtained from the temperature profile was used for the cloud-top temperature. The cloud temperature difference was computed from clear-sky and cloud-contaminated temperatures calculated at identical nadir angles. The range of the nadir angle was $\pm 45°$.

After the total radiance was computed, it was converted into an equivalent blackbody temperature through the relationship derived by the solution of the equation

$$N=\int_{\lambda_1}^{\lambda_2} \phi_\lambda E_\lambda(T) d\lambda \tag{3b}$$

where $E_\lambda(T)$ is Planck's blackbody function. The resulting relationship is well known and can be found in Vukovich and Blanton (1969).

3. MULTILEVEL CLOUD APPROXIMATION

The following describes how the results from the single layer cloud effects computed by the above technique may be used to compute the effect for multilevel clouds. The derivation is presented for two layers of clouds.

If it is assumed that two layers of clouds with percent cloud cover α_1 and α_2, cloud top pressures p_{c1} and p_{c2}, and transmissivities $\tau_{\lambda 1}$ and $\tau_{\lambda 2}$ (which represent the clear sky transmissivities from cloud top to the satellite) obstruct the field of view, then subtracting a multilevel version of eq (1) from the same equation, when $\alpha=0$ (clear skies), yields the following expression for the total difference (TOT ΔN_λ) between the radiation received by the satellite under clear and cloud conditions:

$$\text{TOT } (\Delta N_\lambda)=\phi_\lambda\{\tau_{\lambda 1}\alpha_1[R_{\lambda 1}-E_\lambda(T_{c1})] + (1-\alpha_1)\tau_{\lambda 2}\alpha_2[R_{\lambda 2}-E_\lambda(T_{c2})]\}. \tag{4}$$

The subscript 1 refers to the upper cloud layer. $R_{\lambda 1}$ and $R_{\lambda 2}$ are defined by eq (2) and are the clear-sky radiances at p_{c1} and p_{c2}, respectively.

For a single layer of clouds, the difference (ΔN_λ) between the radiation received by a satellite under clear and cloudy conditions is

$$\Delta N_\lambda=\phi_\lambda\alpha\tau_\lambda'[R_\lambda-E_\lambda(T_c)]. \tag{5}$$

TABLE 1.—*Results of calculations of the cloud temperature difference (°C) with $\alpha=0.2$, 0.4, and 0.6, at cloud-top heights of 1, 3, and 10 km, and zero nadir angle*

Cloud top height	Polar atmosphere	Standard atmosphere	Tropical atmosphere
(km)		$\alpha=0.2$	
1	1.27	1.56	1.11
3	2.68	2.87	2.68
10	4.51	4.55	4.44
		$\alpha=0.4$	
1	2.63	2.94	2.29
3	5.74	5.93	5.72
10	10.18	10.22	10.00
		$\alpha=0.6$	
1	4.06	4.36	3.53
3	9.28	9.48	9.25
10	17.81	17.83	17.43

The combination of eq (4) and (5) yields

$$\mathrm{TOT}(\Delta N_\lambda)=(\Delta N_\lambda)_1+(1-\alpha_1)(\Delta N_\lambda)_2; \quad (6)$$

and integration over the spectral band and multiplication by $\partial T/\partial N$ derived from eq (3b) gives

$$\mathrm{TOT}(\delta T)=(\delta T)_1+(1-\alpha_1)(\delta T)_2. \quad (7)$$

This equation states that the total cloud temperature difference for a two-layer cloud system is equal to the sum of the single layer cloud temperature difference for the upper layer and lower layer where the lower layer value is modified by $(1-\alpha_1)$.

The above procedure was repeated for a three-layer cloud system, and the following equation derived:

$$\mathrm{TOT}(\delta T)=(\delta T)_1+(1-\alpha_1)(\delta T)_2+(1-\alpha_1)(1-\alpha_2)(\delta T)_3 \quad (8)$$

where the subscripts 1, 2, and 3 refer to the high-, middle-, and low-cloud layers, respectively. Equations (7) and (8) may be employed, along with the results of the computations for a single layer of clouds, to compute the cloud temperature difference for two- and three-layer cloud systems.

4. RESULTS

Table 1 gives an example of the results of the computations of the cloud temperature difference for the three atmospheres, three cloud top heights (1, 3, and 10 km), and three different percent cloud covers ($\alpha=0.2$, 0.4, and 0.6). The nadir angle was zero in all cases. It is noted that for a given cloud cover and cloud top height, the difference between the cloud temperature difference from one atmosphere to the next is negligible. On the average, the difference is about 0.5°C which is of the order of magnitude of the errors that would result in the model.

The above results are representative of all the calculations made, and they infer that the calculations are, for the most part, independent of atmospheric effects. However, eq (5) indicates that the difference in the radiation received under clear and cloudy skies is proportional to the spectral response, the percent cloud cover, transmissivity from the cloud top to the satellite, and the difference between the radiation at p_c emitted from pressures greater than p_c and the blackbody emission at p_c from the cloud. Accordingly, the cloud temperature difference is strongly tied to the atmosphere and its effects. Apparently, the lapse rate and moisture profiles for each of these atmospheres interact so that for a given spectral response and percent cloud cover, the transmissivity, τ'_λ, is small when $R_\lambda-E_\lambda(T_c)$ is large and τ'_λ is large when $R_\lambda-E_\lambda(T_c)$ is small, yielding approximately the same ΔN_λ for each atmosphere. This would indicate that the results are valid for dry (in terms of total water vapor content), cold, stable atmospheres; relatively moist, moderate, less stable atmospheres; and very moist, warm, near-neutral atmospheres.

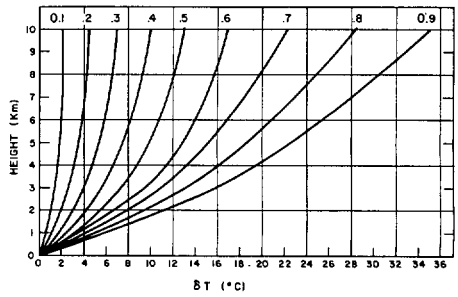

FIGURE 2.—The cloud temperature difference, δT, versus the cloud top height and the cloud cover in tenths (indicated at the end of each curve).

TABLE 2.—*Variation of cloud temperature difference (°C) with nadir angle; $\alpha=0.5$, and cloud top at 3 km*

Nadir angle (deg.)	0	15	30	45
Tropical atmosphere	7.42	7.46	7.58	7.79
Polar atmosphere	7.44	7.46	7.49	7.57
Standard atmosphere	8.00	8.03	8.07	8.16

Table 2 shows an example of the variation of the cloud temperature difference with nadir angle. The calculations are for the three atmospheres with $\alpha=0.5$ and the cloud top at the 3-km altitude. Again, it is noted that there is only a slight variation in the cloud temperature difference for nadir angles between zero and 45 degrees. As before, these data are representative of all the calculations.

Since the variations in the cloud temperature difference with the three atmospheres and the nadir angle employed were negligible, the results were averaged over the three atmospheres and nadir angle. The averaged data are presented in figure 2.

The results show the expected behavior. For a given cloud amount, the temperature difference increases as the cloud top height increases; and for a given cloud top height,

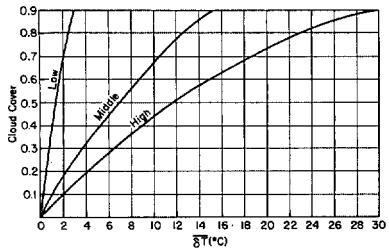

FIGURE 3.—Average cloud temperature difference, $\overline{\delta T}$, versus cloud amount in tenths for low-cloud top height (0 to 1.0 km average), middle-cloud top height (1.0 to 5.0 km average), and high-cloud top height (5.0 to 10.0 km average).

TABLE 3.—*Cloud data used to compute the averaged cloud temperature difference, $\overline{\delta T}$ (°C), from figure 2; and the cloud temperature difference, ΔT (°C), determined from the BOMEX and Nimbus 3 HRIR data*

Date	Latitude (°N)	Longitude (°W)	Cloud type	Cloud amount	$\overline{\delta T}$	ΔT
6/20/69	13	59	towering cumulus (Cu) (high)	0.2	4.2	3.7
6/26/69	13	59	towering Cu (high)	0.2	4.2	3.9
6/26/69	15	56	towering Cu and cumulonimbus (high)	0.2	4.2	4.9
7/11/69	13	54	fracto Cu (low)	0.3	0.9	1.2
7/11/69	15	56	fracto Cu (low)	0.1	4.45*	2.5
			cirrus (high)	0.2		
7/22/69	15	56	towering Cu (high)	0.2	9.5*	9.5
			cirrus (high)	0.3		

*Multilevel computation was employed.

it increases as the cloud amount increases. For cloud tops found at 1 km or below, the cloud temperature difference is small for most cloud amounts. In this case, the cloud-contaminated temperatures would be almost indistinguishable from the clear-sky temperature. It is under this circumstance that cloud-produced variations of the HRIR analyses may be interpreted as real variations, or cloud-contaminated temperatures may be chosen representative of clear-sky values.

It is noted that above 6 km, the cloud temperature difference is almost a constant for 0.1 cloud cover (there are slight differences). The contribution of the surface and atmosphere to N_λ is approximately a constant for a given cloud amount; but the contribution of the cloud depends on cloud top height which is a function of cloud top temperature. As the cloud top height increases (and the cloud top temperature decreases), the contribution of the cloud becomes less significant. Above 6 km and for 0.1 cloud cover, the cloud contribution is insignificant and does not affect the cloud temperature difference to any great extent. As the cloud amount increases, the contribution of the surface and atmosphere becomes smaller, and the cloud contribution eventually may become as significant as the contribution from the clear area.

To use figure 2, we must know the cloud amount and the cloud top height. The latter parameter is not normally observed, though techniques are being developed to estimate the cloud top height from satellite data. Estimation of cloud top height based on cloud type would yield a reasonable estimate of the cloud temperature difference, which might warrant such an approach. The root-mean-square (rms) error that would occur if the cloud temperature difference were averaged from 0 to 1.0 km to represent low-cloud tops, from 1.0 to 5.0 km to represent middle-cloud tops, and from 5.0 to 10 km to represent high-cloud tops, varies from 0.20°C at $\alpha=0.1$ to 2.5°C at $\alpha=0.9$ for low-cloud tops, from 0.12°C at $\alpha=0.1$ to 5.75°C at $\alpha=0.9$ for middle-cloud tops, and from 0°C at $\alpha=0.1$ to 5.29°C at $\alpha=0.9$ for high-cloud tops. The error is smaller than the magnitude of the cloud temperature difference for middle- and high-cloud tops but is about the same order of magnitude for low-cloud tops. The results of the averaging are given in figure 3.

The results in figure 3 were compared with cloud temperature differences computed using Nimbus 3 HRIR data and Barbados Oceanographic and Meterological Experiment (BOMEX) data. The clear sky, equivalent blackbody temperature ($\alpha=0$) in a cloud-contaminated region was computed employing the solution to the radiative transfer equation. The sea-surface temperatures and upper air data obtained during BOMEX were the primary data inputs for the calculations. The cloud-contaminated temperatures were computed from the Nimbus HRIR data. This was done by constructing a frequency diagram using the HRIR temperatures in a one degree latitude-longitude area centered about the point where the clear-sky temperature was computed. The frequency distributions were either Gaussian or Gamma (skewed toward lower temperatures) distributions. Appropriate curve fits were performed on each distribution, and the temperature that was determined to have the highest frequency, from the results of the curve fit, was selected as being most representative of the cloud-contaminated temperature for that area. The difference, ΔT, between the computed clear-sky temperature and statistically determined cloud-contaminated temperature was compared with the average cloud temperature difference, $\overline{\delta T}$ (fig. 3).

Unfortunately, only a small amount of HRIR data was available to make the computations described above. From these data, four cases were found that had a single layer of clouds. Estimates of the degradation produced by multilayer clouds were made through eq (7) and (8).

Table 3 lists the cloud data, the average cloud temperature difference, $\overline{\delta T}$, and the computed cloud temperature difference, ΔT. The differences between $\overline{\delta T}$ and ΔT, for the most part, fell within the combined rms error due to averaging and the error in the radiation calculation, with the exception of the fifth case. In this case, $\overline{\delta T}$ is 2.0°C greater than ΔT. The 0.2 cirrus layer yielded 89 percent of the magnitude of $\overline{\delta T}$. Thin cirrus, which most probably describes the cirrus layer in this case, would yield a reduced cloud temperature difference since it would depart significantly from a blackbody. One should be quite sure that the clouds are significantly dense or thick so that the blackbody assumption will hold when using these results. If the major assumptions do hold, then the cor-

rection factor will account for a large percentage of the effect of partial cloud cover on the 3.8 μm band.

5. SUMMARY AND CONCLUSIONS

A theoretical technique to compute the temperature reduction produced by partial cloud cover, the results of using the technique to compute the cloud temperature difference, and a very limited comparison between the theoretical results and results of computations using Nimbus 3 HRIR data have been described. The comparison, though limited, was encouraging and suggested that the mean cloud temperature difference (fig. 3) could be used as an analysis tool. An estimate of the cloud temperature difference produced by multilayer clouds may be found by using eq (7) and (8) with the results in figure 3.

The calculated curves suggest the possibility of estimating cloud amounts using HRIR data, provided cloud types (low, middle, or high) and an estimate of the clear-sky temperature are known. This is reasonable for single-layer clouds which are opaque. However, an infinite number of solutions would be available in the multilevel cloud case, and the solution for a single-layer cloud is not valid if the cloud departs to a great extent from a blackbody.

ACKNOWLEDGMENT

This research was sponsored, in part, by the National Environmental Satellite Center under Contract No. E-236-69(N). Dr. P. Krishna Rao was Contract Monitor.

REFERENCES

Allison, Lewis J., and Kennedy, James S., "An Evaluation on Sea Surface Temperature as Measured by Nimbus I High Resolution Infrared Radiometers," *NASA Technical Note* No. D-4078, National Aeronautics and Space Administration, Greenbelt, Md., Nov. **1967**, 25 pp.

Bandeen, William R., "Experimental Approaches to Remote Atmospheric Probing in the Infrared From Satellites," *Proceedings of the Scientific Meetings of the Panel on Remote Atmospheric Probing, April-May 1968, Atmospheric Exploration by Remote Probes, Volume 2,* National Academy of Sciences-National Research Council, Washington, D.C., Jan. **1969**, pp. 465–510.

Goddard Space Flight Center, *NIMBUS II User's Guide*, National Aeronautics and Space Administration, Greenbelt, Md., July **1966**, 229 pp.

Krishna Rao, P., "Sea Surface Temperature Measurements From Satellites," *Mariners Weather Log*, Vol. 12, No. 5, Sept. **1968**, pp. 152–154.

Kunde, Virgil G., "Theoretical Relationship Between the Equivalent Blackbody Temperature and Surface Temperature Measured by the NIMBUS High Resolution Infrared Radiometer," *Observations From the NIMBUS I Meteorological Satellite, NASA* SP-89, National Aeronautics and Space Administration, Greenbelt, Md., Dec. **1965**, pp. 23–26.

Vukovich, Fred M., "Physical Oceanography Feasibility Study Utilizing Satellite Data: Part II—Detailed Sea-Surface Temperature Analysis Utilizing NIMBUS HRIR Data," *Final Report*, ESSA Contract No. E-236-69(N), Research Triangle Institute, Research Triangle Park, N.C., Oct. **1970**, 72 pp.

Vukovich, Fred M., and Blanton, Jackson O., "Physical Oceanography Feasibility Study Utilizing NIMBUS II HRIR Satellite Data," *Final Report*, ESSA Contract No. E-256-68(N), Research Triangle Institute, Research Triangle Park, N.C., July **1969**, 133 pp.

[Received December 21, 1970; revised May 26, 1971]